International Journal of Research and Development in Engineering Sciences
ISSN: 2582 - 4201(Online) , http://www.ijrdes.com/
Regular Issue, Vol. 8, Issue. 1 (January – February) , 2026 , Pages: 14 - 34
Received: 14 February 2025 ; *Accepted:* 14 December 2025 ; *Published:* 23 January 2026
https://doi.org/10.63328/IJRDES-V8RI1P3
Original Paper : Applied Research – Experimental Research Paper

Heterogeneous Dual-Channel Edge-Enhanced Temporal Graph Networks with Quantum Optimization for Accurate Schizophrenia Detection

Ramya T [1*], Gopinath M P [2]

[1,2] School of Computer Science and Engineering, Vellore Institute of Technology, Vellore, Tamil Nadu, India ; ramya.t2020@vitstudent.ac.in ; mpgopinath@vit.ac.in

** Corresponding Author: Gopinath M.P ; mpgopinath@vit.ac.in*

Abstract: Schizophrenia (SZ) is a severe neuropsychiatric illness that interferes with cognitive and emotional functioning, making early diagnosis essential. Traditional clinical assessments are often subjective, while EEG signals offer valuable insights but are challenged by high dimensionality, noise, and non-linear patterns. To address these issues, a Novel Heterogeneous Dual-Channel Edge-Enhanced Temporal Graph Convolutional Networks with Quantum-Based Avian Navigation Optimizer (NHDETGCNets+QBANO) is proposed for accurate schizophrenia prediction. The proposed framework begins with the preprocessing of raw EEG signals obtained from the Moscow and Warsaw schizophrenia datasets, employing the Adaptive Self-Guided Loop Filter (AS-GLF) to efficiently suppress noise, artifacts, and other signal distortions while enhancing overall signal quality. Subsequently, informative features are extracted using the Quaternion Quadratic-Phase Fourier Transform Domain (QQ-PFTD), capturing both the temporal and spectral characteristics of the EEG signals. For predictive modeling, the NHDETGCNets architecture is utilized, which seamlessly integrates A Novel Dual-Channel Temporal Convolutional Network (AND-CTCN) with a Heterogeneous Edge-Enhanced Graph Attention Network (HE-EGAN), enabling robust relational modeling across EEG channels. To further optimize performance, the Quantum-Based Avian Navigation Optimizer (QBANO) is employed for dynamic hyperparameter tuning, ensuring faster convergence, minimized error rates, reduced computational overhead, and enhanced scalability. Extensive experimental evaluations demonstrate that the NHDETGCNets+QBANO framework consistently achieves an outstanding prediction accuracy of 99.9%, outperforming existing state-of-the-art approaches and establishing itself as a highly reliable and efficient tool for the early and precise prediction of schizophrenia. The outcomes of the suggested framework provide reliable and precise schizophrenia prediction, accurately distinguishing affected individuals, reducing errors, maintaining consistent performance, and demonstrating robustness and efficiency for early detection.

Keywords: Adaptive Self-Guided Loop Filter, Heterogeneous Edge-Enhanced Graph Attention Network, QQPFTTD .

1. Introduction

With the A severe and long-lasting mental illness, schizophrenia is typified by abnormalities in behavior, emotions, perceptions, and thinking processes [1]. It continues to be one of the most crippling mental illnesses, affecting around 1% of the world's population and frequently resulting in severe impairment in social, vocational, and cognitive functioning. Improving patient outcomes, lowering recurrence rates, and avoiding long-term impairment all depend on early identification and prompt management [2]. The pressing need for objective and trustworthy biomarkers is underscored by the fact that traditional diagnostic methods, which are primarily based on medical interviews and behavioral evaluations, are subjective and prone to variation among practitioners [3]. Since electroencephalography (EEG) is non-invasive, has an excellent temporal resolution, and is reasonably priced, it has become a useful tool for researching brain function. EEG signals capture subtle neural oscillations that reflect underlying brain dysfunction, making them particularly useful for identifying abnormalities associated with schizophrenia [4]. Distinct patterns such as altered event-related potentials, disrupted synchronization, and irregular frequency bands have been reported in patients, suggesting that EEG-based biomarkers can serve as indicators for early diagnosis and prognosis. However, identifying significant patterns in extremely complicated, noisy, and non-linear EEG data is difficult [5–6]. Automating feature extraction and categorization in medical signal processing has become possible due to

ISSN: 2582 - 4201(Online) , http://www.ijrdes.com/ , IJRDES, Vol. 8, Issue 1, 2026 , https://doi.org/10.63328/IJRDES-V8RI1P3

recent developments in computer intelligence, particularly deep learning. Deep learning models can automatically construct structured models from raw data, in contrast to typical machine learning methods, which mostly rely on manually created features [6–8]. This ability to capture complex patterns offers a promising pathway toward highly accurate and scalable schizophrenia prediction systems [9]. Despite these developments, challenges remain in creating deep learning systems for EEG analysis. Significant obstacles include inter-subject variability, the high complexity of EEG signals, and the scarcity of large datasets with labels [10–11].

Moreover, issues such as overfitting, interpretability of deep models, and real-world generalization remain critical barriers to clinical adoption. To address these limitations, researchers are increasingly exploring transfer learning, data augmentation, and explainable AI frameworks, aiming to strike a balance between predictive accuracy and clinical interpretability [12-13]. Additionally, integrating multimodal data sources, such as functional MRI, cognitive tests, and genetic information, with EEG may enhance diagnostic precision. Nevertheless, EEG remains particularly attractive because of its accessibility and suitability for real-time monitoring [14]. Deep learning-powered EEG analysis has the potential to completely transform the early diagnosis and treatment of schizophrenia with continued study, bringing the field one step closer to unbiased, individualized, and therapeutically useful treatments [15].

Existing methods face several challenges, including the use of small datasets, noise, overfitting, poor interpretability, and limited clinical applicability. The study is designed to deal with the recognized challenges.

Novelty as well as contribution

The Novelty as well as the Contribution of the paper is as follows:

- ❖ To develop a robust, scalable, and efficient framework, NHDETGCNets+QBANO, for the precise and early prediction of schizophrenia from multi-channel EEG signals.
- ❖ To preprocess raw EEG signals using the AS-GLF, effectively suppressing noise, removing artifacts, and enhancing the overall signal quality for reliable downstream analysis.
- ❖ To extract comprehensive temporal and spectral features using the QQ-PFTD, capturing subtle non-linear, spatial, and frequency-domain characteristics of brain activity associated with schizophrenia.
- ❖ To perform predictive modeling through NHDETGCNets, this seamlessly integrates AND-CTCN with a HE-EGAN for effective modeling of relational and inter-channel dependencies across EEG channels.
- ❖ To optimize model performance via dynamic and intelligent hyperparameter tuning using the QBANO, minimizing error rates, reducing computational complexity, ensuring scalability, and enhancing robustness. This integrated approach aims to achieve highly accurate, reliable, and interpretable early detection of schizophrenia, thereby promoting neuropsychiatric research and facilitating informed clinical decision-making.

The rest of the manuscript is organized into five sections: Section Two presents the Literature Review, Section Three outlines the Suggested Methods, Section Four covers the Results and Discussion, and Section Five concludes with the Conclusion and Upcoming Projects.

2. Literature Survey

The papers related to neural network-based Accurate Prediction of Schizophrenia are given below:

In 2022, Supakar et al [16] has introduced an RNN-LSTM to diagnose schizophrenia that analyzes EEG signal data. The model, consisting of three thick layers on top of a hundred-dimensional LSTM, was evaluated using EEG data from 45 patients with SZ as well as 39 healthy individuals. With the complete characteristic set, the model's precision was 98%; with the decreased feature set, it was 93.67%. Model performance metrics, along with combined measurements of performance, were used to assess the model's reliability. When assessed against the same data set using CNN or RNN, it outperformed them with the entire dataset and was on par with conventional machine learning classifiers.

In 2022, Sobahi et al [17] has introduced a novel CNN approach to use EEG records for SZ detection. The technique converts EEG input channels into EEG rhythms using wavelet transformations and 1D native binary pattern (LBP) embedded beats. The input EEG signal's channels and columns are used to create the visuals. For data augmentation, autoencoders (AE) based on extreme learning machines (ELM) are employed. The classification of SZ, as well as healthy patients, is done using deep transfer learning using CNN models that have already been trained. Using an EEG database from Lomonosov State University in Moscow, the approach achieves an accuracy score of 97.7%, outperforming other recently reported methods.

In 2022, Sharma et al [18] has presented the SZ heterogeneous neural network (SzHNN), a deep learning model that improves EEG-based Sz prediction in remote

ISSN: 2582 - 4201(Online) , http://www.ijrdes.com/ , IJRDES, Vol. 8, Issue 1, 2026 , https://doi.org/10.63328/IJRDES-V8RI1P3

applications. The model uses convolutional neural networks (CNNs) and long short-term memories (LSTMs) to extract and categorize local information. Its accuracy in classification, at 99.9%, was the highest when compared to other models. Additionally, the model demonstrated improved accuracy with subject-wise testing using just five electrodes, achieving 90.11% and 89.60% accuracy for databases 1 and 2, respectively.

In 2023, Parija, et al [19] has introduced a SCAMBO-MVMKRVFLN technique to identify schizophrenia in EEG data; this combines a multikernel random vector functioning link network with minimum variance with DSEMELMAE. The DSEMELMAE network uses inputs for the SCAMBO-MVMKRVFLN method of classification to extract distinct unsupervised features from brain signals. The method's exceptional classification accuracy, improved computing simplicity, and quicker learning speed make it superior to existing approaches. Using publicly accessible schizophrenia EEG datasets, the technique obtains accuracy levels in classification of 99.989%, 95.012%, and 96.69%.

In 2022, Aslan et al [20] has introduced a VGG16-CNN technique that uses 2D temporal frequency characteristics to automatically identify SZ from EEG recordings. The feature extraction procedure is automated, unlike conventional machine learning techniques. The Visual Geometry Group-16 (VGG16) and CNNs are utilized in the approach to classify SZ patients with an accuracy of 98% and healthy individuals with an accuracy of 99.5%. To depict learning results and differentiate between SZ and healthy individuals, the study used strategies such as Gradient-weighted Class Activation Mapping, Saliency Map, and Activation Maximization.

In 2022, Jindal et al [21] has presented an MSST-Bi-CNN technique for identifying SZ using multichannel EEG stimulation. For precise diagnosis, the system employs a Bi-CNN model based on the multisynthetic transform (MSST). Feature extraction, categorization of decomposed EEG, and 2D time-frequency visualization of EEG activity are all part of the process. The results show that this method is effective for early detection and screening of SZ sickness, with a precision of 84.42%. For early diagnosis, this improvement in medical diagnostics is essential.

In 2023, Grover et al [22] has introduced a Schizo-Net, a very reliable and accurate approach for identifying spinal cord injury (SCZ), which is a late heterogeneous combination of anticipated brain connection indicators using EEG activity. For SCZ in particular, the framework is the first to consider a wide range of brain connectivity metrics. Along with highlighting the significance of the Brain Connection Index (BCI) in finding illness biomarkers, the study identifies abnormalities in the brain connection associated with SCZ. In diagnosing SCZ, Schizo-Net outperforms single-architecture-based predictions with an accuracy of 99.84%. An explanation of the current methods is given in Table 1.

Table. 1 A summary of the current methods

References	Methods	Advantages	Disadvantages
Supakar et al. (2022) [16]	RNN-LSTM	Outperforms CNN/RNN on the same dataset. Robust with combined performance measures.	Computationally heavy (3 thick layers + 100-dim LSTM). Risk of overfitting due to dataset size.
Sobahi et al. (2022) [17]	CNN	Uses data augmentation with AE-ELM to boost robustness. Employs deep transfer learning for generalization.	Requires pretrained CNNs dependency on external models. Performance may vary with different EEG datasets.
Sharma et al. (2022) [18]	SzHNN	Effective with minimal electrodes (5), maintaining ~90% accuracy. Suitable for remote/distant applications.	Validation is limited to only two datasets. Model complexity may hinder deployment on low-resource systems.
Parija et al. (2023) [19]	SCAMBO-MVMKRVFLN	Faster learning speed & reduced computational cost. Superior to existing approaches in simplicity and robustness.	The method is highly specialized, less interpretable. Requires validation on larger, diverse datasets.
Aslan et al. (2022) [20]	VGG16-CNN	Automated feature extraction (no manual engineering). Uses explainability methods (Grad-CAM, Saliency Maps).	VGG16 is computationally expensive. For real-time applications, it might not be effective.

ISSN: 2582 - 4201(Online) , http://www.ijrdes.com/ , IJRDES, Vol. 8, Issue 1, 2026 , https://doi.org/10.63328/IJRDES-V8RI1P3

Jindal et al. (2022) [21]	MSST-Bi-CNN	Introduces Bi-CNN with multichannel EEG analysis. Uses MSST for effective time-frequency decomposition.	Lower accuracy than other models. Performance gap compared to state-of-the-art approaches.
Grover et al. (2023) [22]	Schizo-Net	First to integrate diverse brain connection indices. Identifies brain connectivity abnormalities (biomarker potential).	Model complexity (multimodal integration). May require large, multimodal datasets not always available.

Problem statement

Early and precise diagnosis is essential for successful treatment and management of schizophrenia, a complex neuropsychiatric illness that severely compromises cognitive and functional abilities. Subjective evaluations and variations in clinical symptoms frequently pose challenges to traditional diagnostic techniques. EEG signals have several drawbacks, including high dimensionality, spatial complexity, and noise interference, but they can offer important insights into brain function. To tackle these issues, this study proposes a hybrid optimized deep learning algorithm, leveraging Novel Heterogeneous Dual-Channel Edge-Enhanced Temporal Graph Convolutional Networks with Quantum-Based Avian Navigation Optimizer (NHDETGCNets+QBANO), to enhance prediction accuracy, reduce error rates, and minimize computational complexity.

3. Proposed Methodology

This study proposes a comprehensive and resilient framework, termed **A Novel Heterogeneous Dual-Channel Edge-Enhanced Temporal Graph Convolutional Networks with Quantum-Based Avian Navigation Optimizer (NHDETGCNets+QBANO)**, for the precise and reliable prediction of schizophrenia. The framework is meticulously structured as a **five-phase diagnostic pipeline**, specifically engineered to systematically enhance classification accuracy and clinical reliability. The sequential phases are as follows: (1) Signal Acquisition – acquisition of raw EEG signals sourced from both the Moscow as well as Warsaw schizophrenia EEG benchmark datasets, ensuring cross-cohort diversity; (2) Preprocessing – noise reduction, artifact removal, and normalization of EEG signals for optimal signal quality; (3) Feature Extraction – identifying meaningful temporal, spatial, and frequency-related patterns from the EEG signals; (4) Prediction –to predict both local and global brain connectivity patterns; and (5) Optimization – refining parameters and adjusting the model to achieve the highest level of predictive accuracy. As shown in **Figure 1**, the NHDETGCNets+QBANO architecture illustrates the **end-to-end workflow and data flow**,

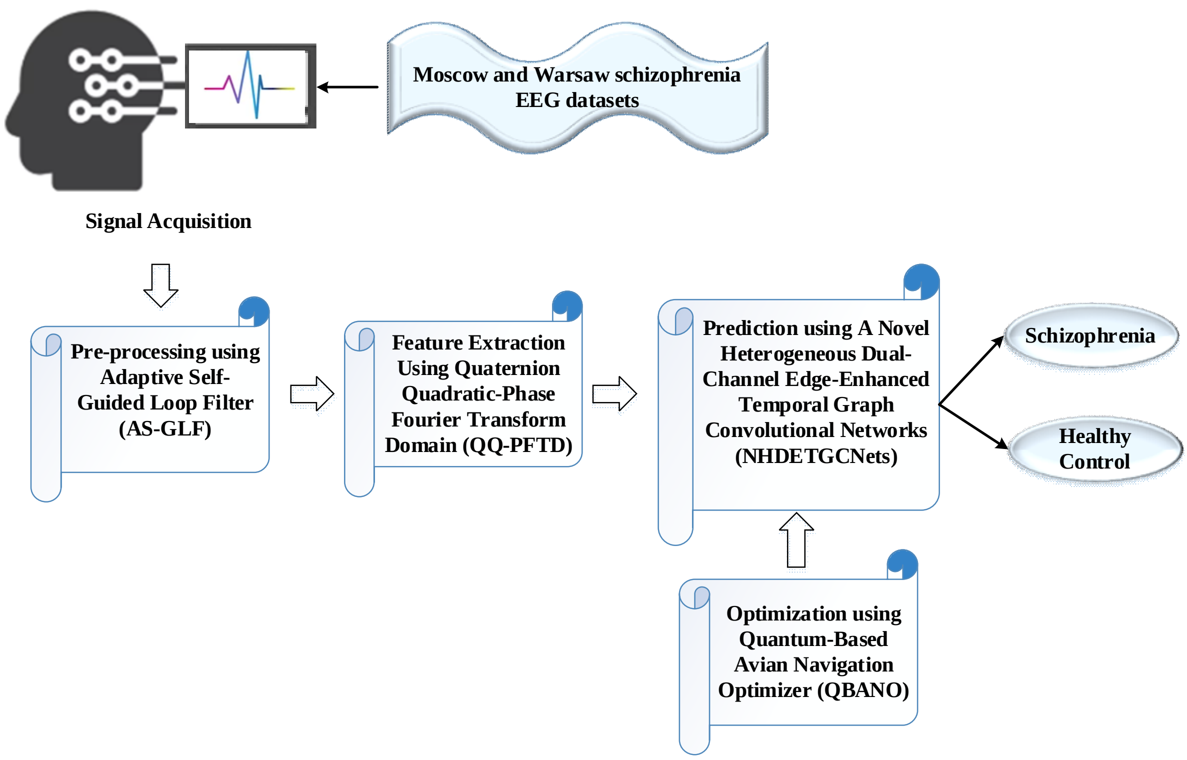

Figure. 1 The complete workflow NHDETGCNets+QBANO architecture

ISSN: 2582 - 4201(Online) , http://www.ijrdes.com/ , IJRDES, Vol. 8, Issue 1, 2026 , https://doi.org/10.63328/IJRDES-V8RI1P3

3.1. Image Acquisition

The input EEG signals are collected from benchmark schizophrenia datasets, including the Moscow and Warsaw cohorts, ensuring diverse subject representation. Although these raw signals are highly prone to noise and artifacts caused by eye blinks, muscle movements, and environmental interference, they do capture neuronal oscillations that are essential for assessing brain activity. As a result, the data undergoes a preprocessing stage, during which methods such as filtering, normalization, and artifact removal are employed. This step ensures high-quality signals, providing a robust foundation for subsequent analysis, as detailed below.

3.2. Pre-processing using Adaptive Self-Guided Loop Filter (AS-GLF)

Preprocessing is the initial data refinement step that removes noise and enhances the signal for analysis. The AS-GLF [23] adaptively smooths EEG signals using edge-aware filtering. It suppresses noise while preserving sharp transitions, ensuring enhanced preprocessing of Moscow and Warsaw schizophrenia EEG datasets for accurate downstream prediction.

EEG data is segmented into blocks (or time–frequency windows). Each block is classified based on **variance** to determine its filtering strength as given by equation (1):

$$un_{block} = clip3(0, un_{ttl} - 1, un_{initi}) \qquad (1)$$

where, un_{initi} is an initial block index, un_{block} is a clipped block index, un_{ttl} is the total number of classes. Blocks with **high variance (rich texture or edges)** get **less filtering**, while smoother blocks get **stronger filtering**.

Each EEG sample at position (p,q) is filtered as a weighted combination of itself and its local neighbourhood mean as given by equation (2):

$$L_{ut}(p,q) = e(p,q) \times L_{in}(p,q) + s(p,q) \times mean_{window}(p,q) \qquad (2)$$

where, $L_{in}(p,q)$ is an input EEG sample at (p,q), $mean_{window}(p,q)$ is a mean within the local filtering window, $e(p,q)$ and $s(p,q)$ are adaptive weights. $L_{ut}(p,q)$ is a filtered output sample.

Weights are determined from **local variance** and **edge-aware factors as given by equation (3)**:

$$s_{initi}(p,q) = 1 - e_{initi}(p,q) \qquad (3)$$

where, $s_{initi}(p,q)$ and $e_{initi}(p,q)$ are the initial weights.

Final weights are obtained by averaging across overlapping windows as given by equations (4 and 5):

$$e(p,q) = \frac{1}{M}\left(\sum_{h=1}^{h=5} e_{initi}(h)\right) \qquad (4)$$

$$s(p,q) = \frac{1}{M}\left(\sum_{h=1}^{h=5} s_{initi}(h)\right) \qquad (5)$$

AS-GLF preprocessing combines block-level variance analysis and local edge-aware filtering. By adjusting weights through adaptive statistical factors, it reduces artifacts, preserves essential EEG oscillations, and significantly improves the reliability of schizophrenia prediction using Moscow State and Warsaw EEG datasets. After AS-GLF preprocessing, the **denoised and edge-preserved EEG signals** are fed into the **feature extraction process.**

3.3. Feature Extraction Using Quaternion Quadratic-Phase Fourier Transform Domain (QQ-PFTD)

The extraction of features is the process of transforming unstructured data into useful, condensed representations that capture essential patterns for analysis. The **QQ-PFTD** [24] extends the standard Quaternion Fourier Transform (QFT) by introducing **quadratic phase modulation**, allowing better capture of **time–frequency–phase variations** in multi-channel EEG signals. This makes it well-suited for analyzing the **non-stationary EEG activity** observed in schizophrenia.

For an EEG signal $j(l)$, the QQPFT is defined as equation (6):

$$\left(O_K^{\wedge_1,\wedge_2} j\right)(\alpha) = \frac{1}{2\hbar}\int_{P^2} s^{-a(X_1 j_1^2 + Y_1 l_1 \alpha_1 + Z_1 \alpha_1^2 + W_1 l_1 + U_1 \alpha_1)}\, j(l)\, s^{-b(X_2 l_2^2 + Y_2 l_2 \alpha_2 + Z_2 \alpha_2^2 + W_2 l_2 + U_2 \alpha_2)}\, dl \qquad (6)$$

where, $j = (j_1, j_2)$ is a time variables (2D time coordinates), $\alpha = (\alpha_1, \alpha_2)$ is a frequency variables corresponding to j_1, j_2, $\left(O_K^{\wedge_1,\wedge_2} j\right)(\alpha)$ is a EEG signal in QQ-PFTD of $j(l)$, X_1 and X_2 are a Quadratic coefficients (control curvature in time), Y_1 and Y_2 are a time–frequency scaling factors (must be nonzero), Z_1 and Z_2 are a quadratic coefficients in frequency domain (frequency curvature), W_1 and W_2 are a linear phase shift coefficients (time), U_1 and U_2 are a linear phase shift coefficients (frequency).

From the transformed EEG signals, features are extracted as **energy features (Parseval's relation) as given by equation (7):**

$$\|j\|^2_{T_K^2(P^2)} = |Y_1 Y_2| \left\|O_K^{\wedge_1,\wedge_2} j\right\|^2_{T_K^2(P^2 \times P^2)} \qquad (7)$$

where, $\|j\|^2_{T_K^2(P^2)}$ is a quaternion $T_K^2(p^2)$ -norm (energy/complexity measure), $|Y_1Y_2|$ is a normalization/scaling factor in inversion and Parseval formulas. These entropies provide **complexity measures** of EEG signals.

The **QQ-PFTD** maps raw EEG signals into a **quadratic-phase quaternion spectral space**, from which **energy, entropy, and statistical features** are extracted. These features, when applied to Moscow and Warsaw schizophrenia EEG datasets, provide **highly discriminative biomarkers**, ensuring **accurate schizophrenia prediction**. The extracted features are input into NHDETGCNets, enabling the accurate prediction of schizophrenia versus healthy controls.

3.4. Prediction using A Novel Heterogeneous Dual-Channel Edge-Enhanced Temporal Graph Convolutional Networks (NHDETGCNets)

After feature extraction, prediction is performed using the NHDETGCNets framework, which integrates an AND-CTCN with HE-EGAN. To further improve accuracy in Schizophrenia prediction, A Novel Heterogeneous Dual-Channel Edge-Enhanced Temporal Graph Convolutional Networks (NHDETGCNets) model is proposed. This offers a robust and comprehensive solution, summarized as follows:

3.4.1. A Novel Dual-Channel Temporal Convolutional Network (AND-CTCN)

The AND-CTCN [25] model predicts schizophrenia from EEG signals using a dual-channel structure. The **Moscow State University** and **Warsaw Schizophrenia EEG datasets** are used for predicting schizophrenia. Each channel processes temporal patterns independently, and their outputs are concatenated. The fused features are passed to a prediction layer with softmax activation to determine whether an individual has schizophrenia or a healthy status.

At each time i, the EEG input is given by equation (8):

$$\hat{Z}_i = \{\tilde{z}_1, \tilde{z}_2, \tilde{z}_3, \ldots\ldots, \tilde{z}_i\} \in Q_{i\times 2}$$
(8)

where, $\hat{Z}_i$ is an EEG input at time i, Q is the number of EEG channels, $\tilde{z}_i$ is an EEG signal from channel at time i.

The EEG sequence is simultaneously processed by two independent TCN channels, where Channel 1 captures temporal patterns associated with schizophrenia-related neural activities, while Channel 2 extracts complementary patterns to enhance overall discrimination.

Predicted outputs of both channels are combined as equation (9):

$$\tilde{z}_i = (\tilde{z}_S, \tilde{z}_F) \qquad (9)$$

where, $\tilde{z}_S$ is an output of Channel 1, $\tilde{z}_F$ is an output of Channel 2, $\tilde{z}_i$ is a fused representation of both channels. The fused vector is mapped to the output space through a prediction layer as given by equation (10):

$$Z^{(k)} = \xi\left[G(Z^{(k-1)}) + Z^{(k-1)}\right] \qquad (10)$$

where, $Z^{(k)}$ is a predicted class (0 = healthy, 1 = schizophrenia), $G(Z^{(k-1)})$ is a weight parameter of the prediction layer, $Z^{(k-1)}$ is a bias parameter, $\xi[\cdot]$ is a softmax activation function.

Schizophrenia prediction is achieved through EEG input modeling using AND-CTCN. Two temporal channels capture distinct brain activity patterns, which are fused and mapped to an output layer. The model directly classifies subjects as schizophrenia patients or healthy controls, ensuring accurate diagnostic prediction.

3.4.2. Heterogeneous Edge-Enhanced Graph Attention Network (HE-EGAN)

EEG is represented as a heterogeneous structure using HE-EGAN [26], in which electrodes serve as nodes and connection edges represent interactions. Type-specific encoders, edge-enhanced attention, and gated brain priors extract dynamic features, enabling accurate prediction of schizophrenia across Moscow and Warsaw EEG datasets. For schizophrenia EEG data, the EEG channels/subjects act as heterogeneous agents, and their interactions (functional connectivity, coherence, etc.) form a heterogeneous edge-featured graph.

The input at time l as given by equation (11):

$$W_l = [\mathrm{N}_l, \Xi] \qquad (11)$$

where, $\mathrm{N}_l = \{n_l^1, n_l^2, \ldots, n_l^m\}$ historical EEG states of m electrodes/patients, Ξ is an auxiliary context (could be a brain region map).

The output: predicted **schizophrenia state trajectory** (healthy vs patient) as given by equation (12):

$$R_l = \{r_l^1, r_l^2, \ldots\ldots, r_l^w\} \qquad (12)$$

Each EEG sequence is passed through a type-specific encoder (for different electrode regions or dataset sources) as given by equations (13 and 14):

$$s_l^a = GRU_{hst}^{\varsigma}(n_l^a) \qquad (13)$$

ISSN: 2582 - 4201(Online) , http://www.ijrdes.com/ , IJRDES, Vol. 8, Issue 1, 2026 , https://doi.org/10.63328/IJRDES-V8RI1P3

$$G_l = \{s_l^1, s_l^1, ..., s_l^m\} \quad (14)$$

where, s_l^a is a dynamic feature of the electrode/region a, ς is a type (dataset/patient group/EEG region), G_l is the all nodes' features. EEG electrodes/patients are nodes; their correlations are edges. Interaction features extracted with HE-EGAN (HEAT) are given by equation (15):

$$O_l = \{o_l^0, o_l^1, ..., o_l^m\} = HEAT_{en}(P_l, F_l) \quad (15)$$

where, F_l is an edge set (EEG connectivity, coherence, mutual information), o_l^m is an interaction feature of a node n.

Final classification/prediction uses agent-type-specific predictor as given by equation (16):

$$y_l^a = lstm_{future}^{\varsigma}(\left[s_l^a \| d_l^a \| n_l^a\right]) \quad (16)$$

HE-EGAN leverages edge-aware attention to integrate connectivity and temporal EEG features. Node embeddings are aggregated into graph-level representations for classification. Applied to Moscow and Warsaw schizophrenia EEG datasets, it achieves a reliable distinction between schizophrenia patients and healthy controls with enhanced accuracy.

NHDETGCNets integrates AND-CTCN with HE-EGAN, capturing multi-type brain connectivity. Fusing temporal and graph features enables robust classification, achieving accurate schizophrenia prediction on Moscow State University and Warsaw EEG datasets. The QBANO algorithm enhances the NHDETGCNets framework by lowering computational cost, complexity, error rate, and execution time, while boosting detection accuracy. Its optimization process follows the key stages outlined below:

3.5. Optimization using Quantum-Based Avian Navigation Optimizer (QBANO)

QBANO optimizes the weight parameters of the NHDETGCNets model to improve overall performance, while bias correction reduces processing time, error rate, computational complexity, and costs. The QBANO [27] mimics bird navigation using quantum strategies to optimize the hyperparameters of NHDETGCNets by combining bird-inspired flocking, quantum mutation, and qubit crossover. It balances exploration and exploitation, evaluates fitness with accuracy and complexity, and converges efficiently to optimal solutions for robust EEG classification performance. Figure 2 presents the QBANO workflow, with each phase explained below.

Step1: Initialization

Population of candidate hyperparameters is initialized randomly as given by equation (17):

$$\varpi_K(l+1) = C_a(l) \times y_{bst} + (lo + (up - lo) \times rand(0,1)) \quad (17)$$

where, $C_a(l)$ is a position vector of the a^{th} bird/agent at iteration l (candidate hyperparameters), up and lo are the lower and upper bounds of hyperparameters. The population is divided into multiple flocks with a V-echelon topology: a header (leader), left-line birds, and right-line birds.

Step 2: Random Generation

Candidate hyperparameter vectors are initialized randomly in continuous space, and then converted to binary for discrete parameters using a threshold or transfer function, enabling hybrid exploration of continuous and discrete NHDETGCNets hyperparameters.

Step 3: Evaluation of Fitness Function

The fitness function is designed to improve model performance by simultaneously maximizing accuracy and minimizing the error rate, as shown in equation (18):

$$fts_n = \min imize\left(Z^{(k-1)}\right)\max imize\left(G(Z^{(k-1)})\right) \quad (18)$$

where, $G(Z^{(k-1)})$ is to maximize accuracy, while $Z^{(k-1)}$ minimizing error rate, computational cost, runtime, and model complexity.

Step 4: Exploration Phase (Quantum-Based Navigation)

Exploration utilizes quantum-inspired mutations to probabilistically move agents, taking into account both short-term and long-term memory, as well as neighbors, thereby enabling a wide search of the hyperparameter space to avoid local optima.

Exploration is guided by two mutation techniques as **given by equations (19 and 20)**:

$$\varpi_a(l+1) = y_{bst}(l) + C_a(l) \times (y_{vech}(l) - y_{t\in LM}(l)) + C_a(l) \times (y_{vech}(l) - y_{bst}(l)) + C_a(l) \times (y_{t\in LM}(l) - y_{t\in SM}(l)) \quad (19)$$

$$\varpi_a(l+1) = C_a(l) \times (y_{bst}(l) - y_{vech}(l)) + C_a(l) \times (y_{bst}(l) - y_{t\in L} \quad (20)$$

where, $C_a(l)$ is a quantum orientation, $y_{vech}(l)$ is an echelon neighbor, $y_{t\in LM}(l)$ and $y_{t\in SM}(l)$ are the samples from long/short-term memory, $y_{bst}(l)$ is the best solution found so far.

Step 5: Exploitation Phase (Qubit-Crossover & Update)

ISSN: 2582 - 4201(Online) , http://www.ijrdes.com/ , IJRDES, Vol. 8, Issue 1, 2026 , https://doi.org/10.63328/IJRDES-V8RI1P3

Exploitation utilizes qubit-based crossover to probabilistically combine parent and mutant solutions, fine-tuning hyperparameters around promising candidates for NHDETGCNs, thereby improving accuracy while reducing error and computational cost.

Crossover combines parents and mutants given by equation (21):

$$\pi_{ag}(l+1)=\begin{cases} y_{ag}(l-1), & |\vartheta_a\rangle_g \geq rand \\ \varpi_{ag}(l-1), & |\vartheta_a\rangle_g < rand \end{cases}$$

(21)

This allows **probabilistic switching** between solutions for fine-tuning hyperparameters.

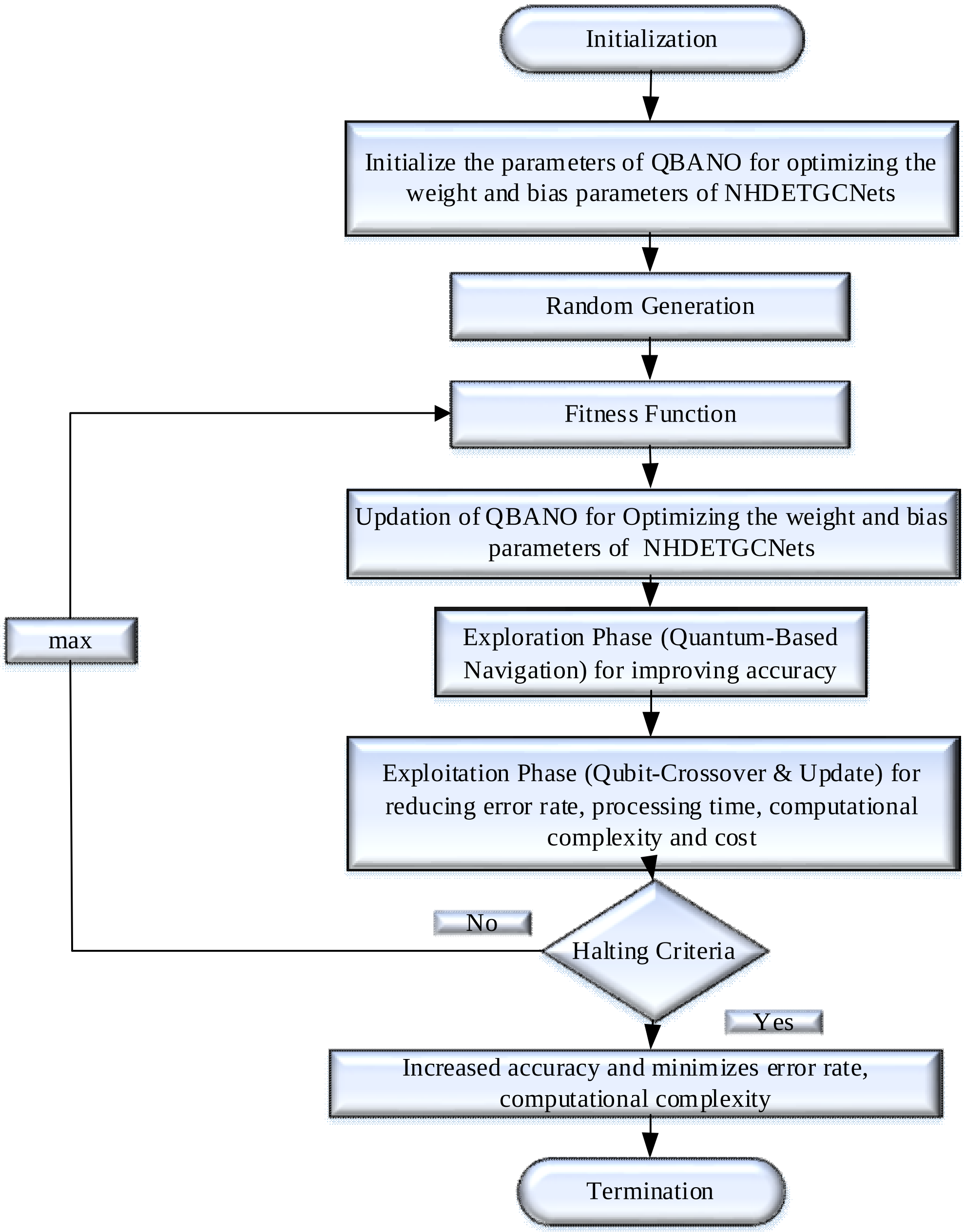

Figure. 2 The QBANO process

Step 6: Termination

Termination occurs when the maximum iterations $(\max)$are reached or the fitness of the best solution falls below the threshold.

This study presents a new framework, **A Novel Heterogeneous Dual-Channel Edge-Enhanced Temporal Graph Convolutional Networks with Quantum-Based Avian Navigation Optimizer (NHDETGCNets+QBANO)**, developed to achieve highly accurate prediction of schizophrenia. The methodology begins with **AS-GLF–based preprocessing**, which refines and enhances raw EEG signals to improve data quality. Next, **QQ-PFTD–based feature extraction** is employed to capture intricate patterns from the processed signals. These extracted features are then passed through the **NHDETGCNets architecture** to provide robust and reliable predictive modeling. To further fine-tune performance, the

ISSN: 2582 - 4201(Online) , http://www.ijrdes.com/ , IJRDES, Vol. 8, Issue 1, 2026 , https://doi.org/10.63328/IJRDES-V8RI1P3

predictions are optimized using the **QBANO**, ensuring higher precision and generalization capability. Comprehensive experimental evaluations, along with an in-depth explanation of the results, are presented in the subsequent section.

4. Experimental Results and Discussions

This section presents the findings and discussion of the NHDETGCNets+QBANO model, developed in Python. The key implementation parameters are summarized in Table 2.

Table. 2 Implementation Parameters

Parameters	Description
Programming Language	Python
Version	3.7.14
OS	Windows 10
Proposed Neural Network	NHDETGCNets
Optimization	QBANO
Datasets	Moscow and Warsaw schizophrenia EEG datasets

3.6. Dataset Description

This section presents a thorough summary of accurate schizophrenia prediction, with a particular focus on the Moscow and Warsaw schizophrenia EEG datasets. The following subsection offers a thorough explanation of these datasets.

3.6.1. Moscow Schizophrenia EEG dataset

This study utilized the EEG Schizophrenia Database, which is openly accessible and originates from the Laboratory for Neurophysiology and Neuro-Computer Interface at Lomonosov Moscow State University. It includes EEG recordings from 84 teenagers between the ages of 11 and 14 (mean age 12.3), 45 of whom have been diagnosed with SZ, while 39 of whom are healthy controls. Every participant satisfied the ICD-10 diagnostic criteria for schizophrenia after being evaluated at the Mental Health Research Center (MHRC). A 16-channel electrode configuration in accordance with the 10–20 international standard (O1, O2, P3, P4, Pz, T5, T6, C3, C4, Cz, T3, T4, F3, F4, F7, F8) was used to capture EEG data while the subjects were at rest with their eyes closed. At a sampling rate of 128 Hz, all recordings lasted 60 seconds and yielded 7680 measurements per channel, which were then saved in conventional ASCII format. Preprocessing was performed to ensure signal quality and consistency, involving the application of z-score normalization, bandpass filtering within the 4–45 Hz range, and manual artifact removal. 20% of the dataset was used for testing, while the remaining 80% was used for training. The example output photos from this dataset are shown in Figure 3.

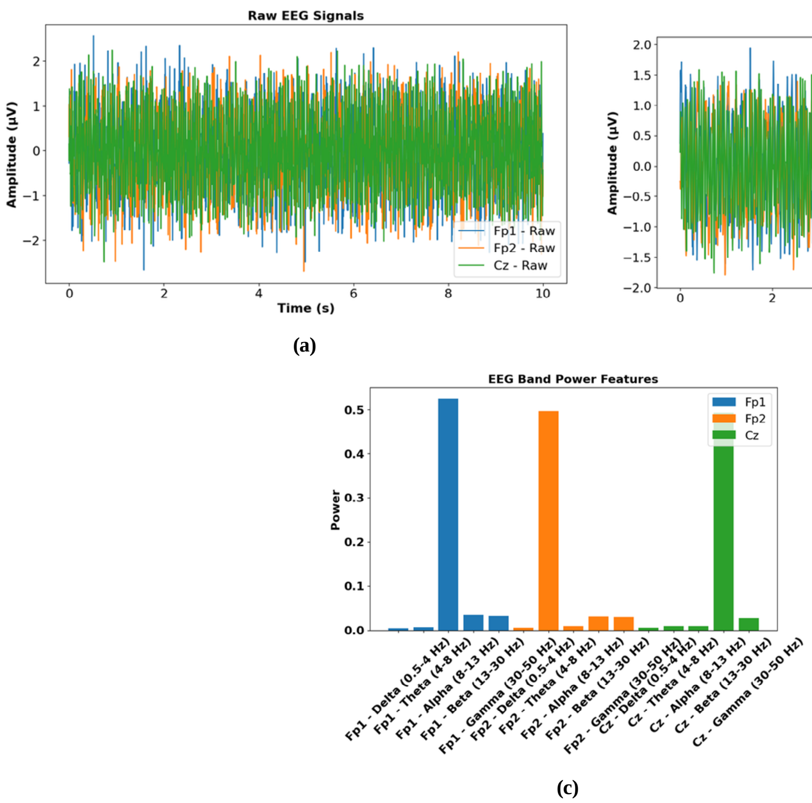

Figure. 3 The sample output images result from the Moscow Schizophrenia EEG dataset (a) Raw EEG Signals, (b) Preprocessed EEG Signals, and (c) EEG Band Power Features

ISSN: 2582 - 4201(Online) , http://www.ijrdes.com/ , IJRDES, Vol. 8, Issue 1, 2026 , https://doi.org/10.63328/IJRDES-V8RI1P3

3.6.2. Warsaw Schizophrenia EEG dataset

EEG signals from 14 patients with paranoid schizophrenia (seven men and seven females, mean ages 27.9 ± 3.3 as well as 28.3 ± 4.1 years, respectively), along with 14 healthy controls who were matched for age and gender, were recorded. The Institute of Psychiatry and Neurology in Warsaw, Poland, is making the dataset publicly accessible, and all subjects provided their informed consent. Following the usual International 10–20 system, a 19-channel setup was used to collect EEG data. The Fp1, Fp2, F7, F3, Fz, F4, F8, T3, C3, Cz, C4, T4, T5, P3, Pz, P4, T6, O1, along with O2 channels were all referred to FCz. For 15 minutes, recordings were made at a sampling rate of 250 Hz while the subjects were at rest and had their eyes closed. Independent Component Analysis (ICA) was used to denoise the data, and a 50 Hz notch filter was used to eliminate power-line interference. 20% of the dataset was used for testing, while the remaining 80% was used for training. Figure 4 presents the sample output image results from this dataset,

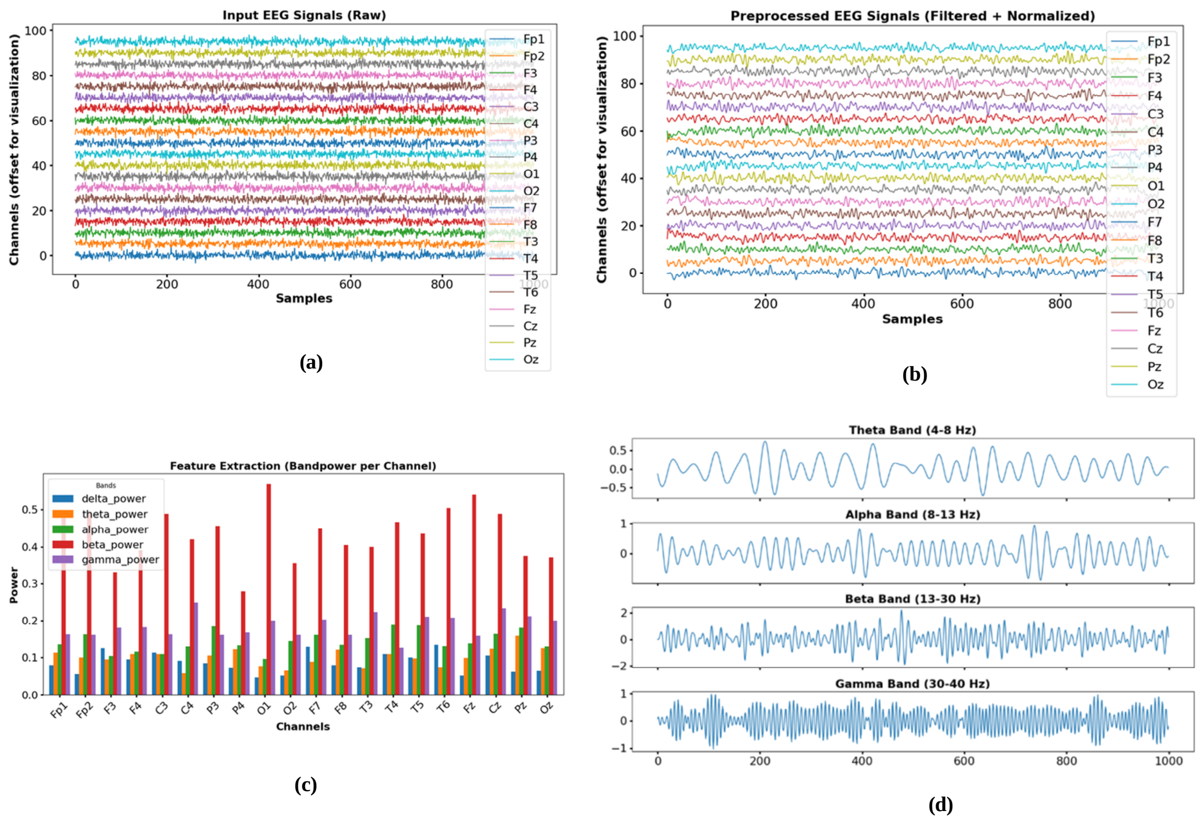

Figure 4: The sample output images result from the Warsaw Schizophrenia EEG dataset, (a) Input EEG Signals (Raw), (b) Preprocessed EEG Signals (Filtered + Normalized), (c) Feature Extraction (Bandpower per Channel), and (d) EEG Frequency Bands

3.7. Performance metrics

The suggested NHDETGCNets+QBANO method is benchmarked against several cutting-edge models. The comparison for the Moscow Schizophrenia EEG database consists of RNN-LSTM [16], CNN [17], SzHNN [18], and SCAMBO-MVMKRVFLN [19]. In the case of the Warsaw Schizophrenia EEG dataset, the baseline models are SzHNN [18], SCAMBO-MVMKRVFLN [19], VGG16-CNN [20], and MSST-Bi-CNN [21]. The evaluation framework incorporates a comprehensive set of performance metrics, namely computational time, precision, accuracy, specificity, recall, sensitivity, error rate, and F1-score. Formal mathematical definitions of these indicators are summarized in Table 3, while their derivations and detailed interpretations are elaborated in the subsequent sections.

True Positive $(tr_\Diamond)$ **:** Correctly identifies early signs of schizophrenia from EEG patterns when schizophrenia is actually present.

False Positive $(fa_\Diamond)$ **:** Incorrectly indicates schizophrenia from EEG patterns when schizophrenia is not present.

False Negative (fa_∇) **:** Fails to detect schizophrenia from EEG patterns when schizophrenia is actually present.

True Negative (tr_∇) **:** Correctly identifies no signs of schizophrenia from EEG patterns when schizophrenia is not present.

ISSN: 2582 - 4201(Online) , http://www.ijrdes.com/ , IJRDES, Vol. 8, Issue 1, 2026 , https://doi.org/10.63328/IJRDES-V8RI1P3

Table 3: Performance metrics as well as the equation

Performance metrics	Equations (22-27)
Accuracy	$\frac{tr_{\Diamond} + tr_{\nabla}}{tr_{\Diamond} + tr_{\nabla} + fa_{\Diamond} + fa_{\nabla}}$ (22)
Precision	$\frac{tr_{\Diamond}}{tr_{\Diamond} + fa_{\Diamond}}$ (23)
Recall	$\frac{tr_{\Diamond}}{tr_{\Diamond} + fa_{\nabla}}$ (24)
Specificity	$\frac{tr_{\nabla}}{tr_{\nabla} + fa_{\Diamond}}$ (25)
Sensitivity	$\frac{tr_{\Diamond}}{tr_{\Diamond} + fa_{\nabla}}$ (26)
F1-score	$\frac{2 \times (pn_{\cap} \times re_{\mathfrak{Z}})}{pn_{\cap} + re_{\mathfrak{Z}}}$ (27)

where, $pn_{\cap}$ represents the precision as well as $re_{\mathfrak{Z}}$ represents the recall.

3.8. Performance analysis of suggested methods

The performance of the NHDETGCNets+QBANO method is assessed in this section.

3.8.1. Performance analysis of the Moscow Schizophrenia EEG dataset

The assessment results for the Moscow Schizophrenia EEG dataset are presented below, with Table 4 providing a comparison of the proposed method's performance on this dataset.

Table. 4 Performance comparison of the suggested approach on the Moscow Schizophrenia EEG dataset

Metrics / Methods	RNN-LSTM [16]	CNN [17]	SzHNN [18]	SCAMBO-MVMKRVFLN [19]	NHDETGCNets+QBANO (Proposed)
Accuracy (%)	91.6	95.2	93.1	94.5	**99.9**
Sensitivity (%)	90.3	93.1	91.6	89.5	**99.8**
Specificity (%)	92.1	94.6	88.2	91.6	**99.8**
Precision (%)	91.5	85.4	94.9	92.9	**99.8**
Recall (%)	90.3	93.9	88.9	91.9	**99.8**
F1- score (%)	90.4	82.7	91.6	92.9	**99.8**

Table 4 presents a performance comparison of various models on the Moscow Schizophrenia EEG dataset. Traditional models, such as RNN-LSTM, CNN, SzHNN, and SCAMBO-MVMKRVFLN, achieved accuracies ranging from 91.6% to 95.2%. However, the proposed NHDETGCNets+QBANO model significantly outperformed them, attaining 99.9% accuracy, sensitivity, recall, and F1-score, along with 99.8% specificity and precision. These findings demonstrate the suggested hybrid approach's resilience and excellence in managing intricate EEG data, ensuring a minimal error rate, higher precision, and reliable classification for schizophrenia prediction compared to existing methods. Figure 5 shows the (a) Confusion and (b) Correlation Matrices,

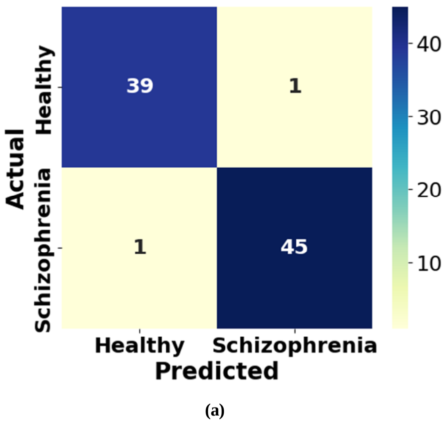

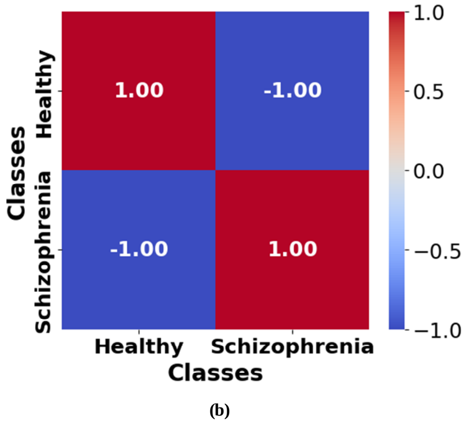

Figure. 5 The (a) Confusion; (b) Correlation Matrices

ISSN: 2582 - 4201(Online) , http://www.ijrdes.com/ , IJRDES, Vol. 8, Issue 1, 2026 , https://doi.org/10.63328/IJRDES-V8RI1P3

Figure 5(a) shows the confusion matrix representing the classification results between healthy individuals and schizophrenia patients. Out of the total samples, the model correctly classified 39 healthy and 45 schizophrenia cases, with only one misclassification in each class, demonstrating strong predictive accuracy.

Figure 5(b) presents the correlation matrix of the two classes, where the diagonal values are +1.00, indicating that each class has a perfect correlation with itself. However, the off-diagonal values are -1.00, representing a complete negative correlation between the healthy and schizophrenia groups. Figure 6 shows the comparison of Feature1 distributions,

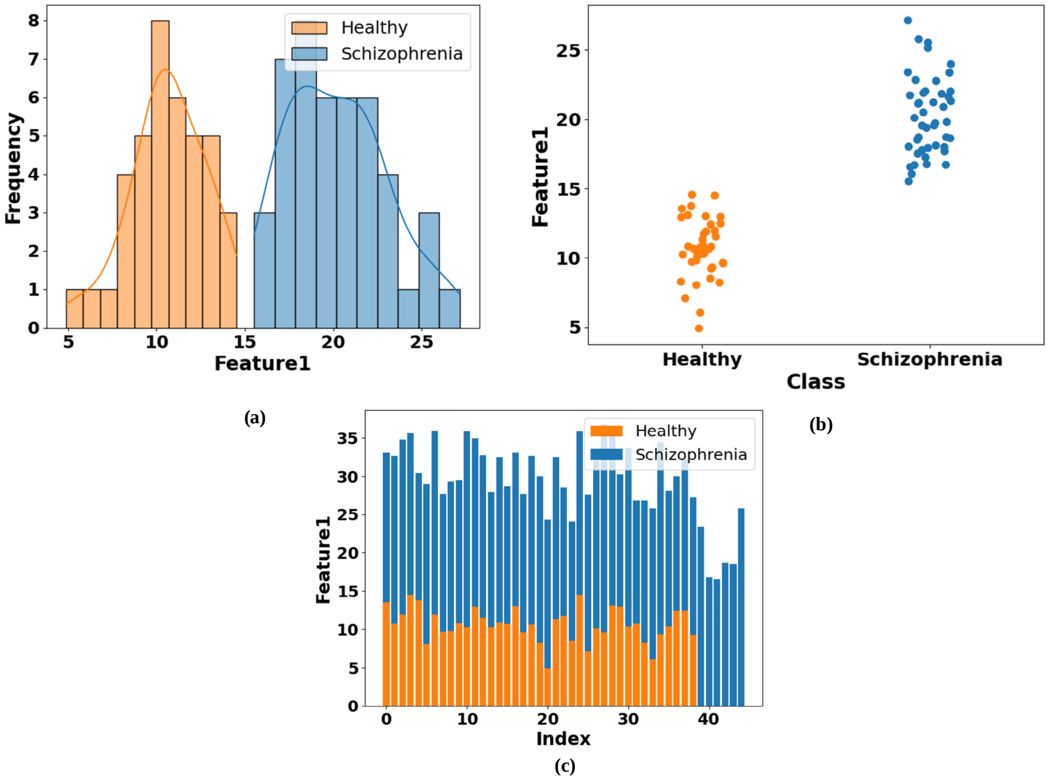

Figure. 6 Comparison of Feature1 distributions: (a) histogram, (b) scatter, (c) bar

Figure 6 illustrates the variations in Feature1 between healthy and schizophrenia groups using three visualization methods. Subfigure (a) displays a histogram with density plots, highlighting distinct distribution patterns where healthy subjects cluster around lower Feature1 values, while schizophrenia patients exhibit a higher range. Subfigure (b) presents a scatter plot, clearly separating the two classes, with healthy individuals grouped between 8 and 13 and schizophrenia patients spread across 15 and 25. Subfigure (c) displays a bar chart across sample indices, highlighting consistent differences where schizophrenia values consistently remain higher than those of healthy individuals. Collectively, these plots demonstrate clear separability between groups based on Feature1. Figure 7 shows the feature comparisons between groups.

Figure 7 shows a comparative analysis of healthy and schizophrenia groups using different plots. Subfigure (a) presents a scatter plot of Feature1 versus Feature2, where schizophrenia samples consistently show higher values than healthy ones, forming two distinct linear clusters. Subfigure (b) depicts violin plots for Feature1, indicating that healthy individuals have lower, narrowly distributed values, while schizophrenia patients exhibit higher, broader distributions. Subfigure (c) uses line plots across indices, reinforcing the consistent difference, with schizophrenia values maintaining a higher trend relative to healthy values. Together, these visualizations demonstrate a strong separability of classes based on Feature1 and Feature2. Figure 8 displays the (a) distribution of classes as well as (b) feature ECDF comparison.

Figure 8(a) displays the distribution of classes between the healthy and schizophrenia groups, indicating nearly balanced samples, with slightly more schizophrenia cases. This balance is important for fair model training and unbiased evaluation. Figure 8 (b) illustrates the ECDF of Feature1 for both classes. It reveals a clear separation, where healthy individuals cluster around lower values, while schizophrenia cases align with higher values. Such distinct patterns suggest that Feature1 has potential discriminative power for effectively distinguishing between the two groups. Figure 9 shows the (a) ROC Curve, (b) PR Curve, (c) Error Rate Comparison,

ISSN: 2582 - 4201(Online) , http://www.ijrdes.com/ , IJRDES, Vol. 8, Issue 1, 2026 , https://doi.org/10.63328/IJRDES-V8RI1P3

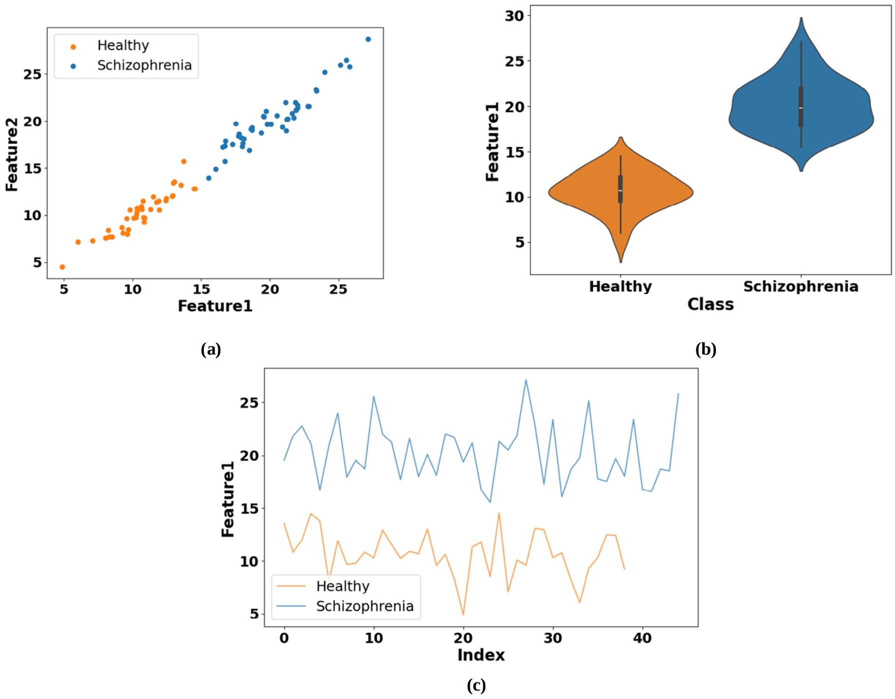

Figure. 7 Feature comparisons between groups: (a) scatter, (b) violin, (c) line

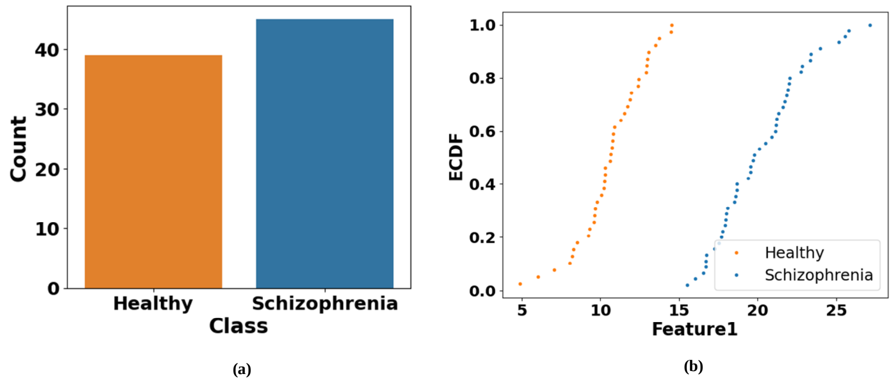

Figure. 8 (a) Distribution of classes and (b) feature ECDF comparison

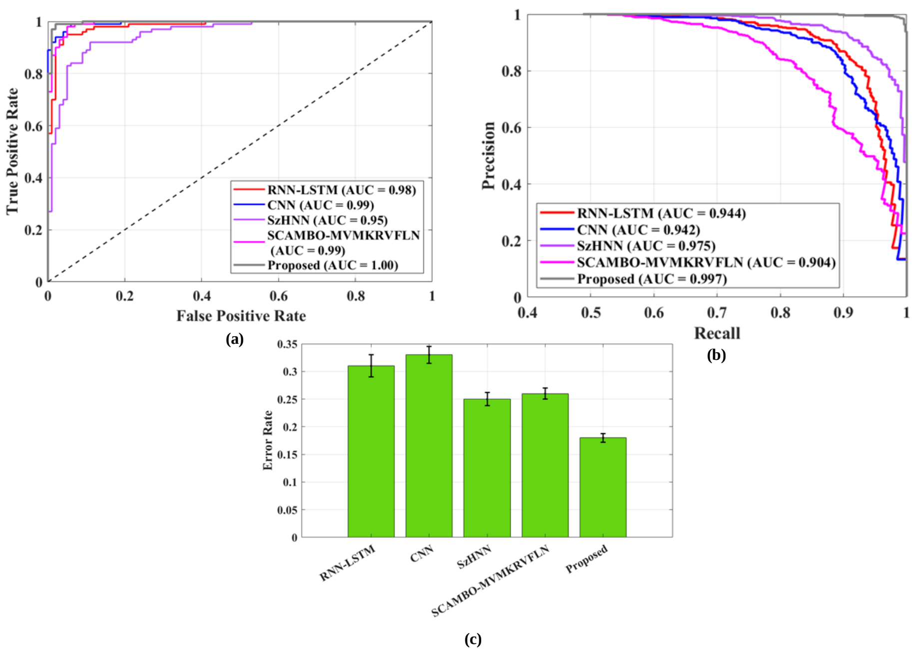

Figure. 9 (a) ROC Curve, (b) PR Curve, (c) Error Rate Comparison

ISSN: 2582 - 4201(Online) , http://www.ijrdes.com/ , IJRDES, Vol. 8, Issue 1, 2026 , https://doi.org/10.63328/IJRDES-V8RI1P3

Figure 9 illustrates the performance evaluation of various models, including RNN-LSTM, CNN, SzHNN, SCAMBO-MVMKRVFLN, and the proposed model. Subfigure (a) displays the ROC curve, which achieves a maximum AUC of 1.00 using the suggested model, demonstrating superior classification capability. The accuracy-recall (PR) curve is shown in Subfigure (b), where the suggested model performs better than the others once more, with an AUC of 0.997, indicating an improved balance of accuracy and recall. Subfigure (c) illustrates the error rate comparison, where the proposed model exhibits the lowest error rate, underscoring its effectiveness and reliability in comparison to traditional and existing methods. Figure 10 shows the training as well as testing performance,

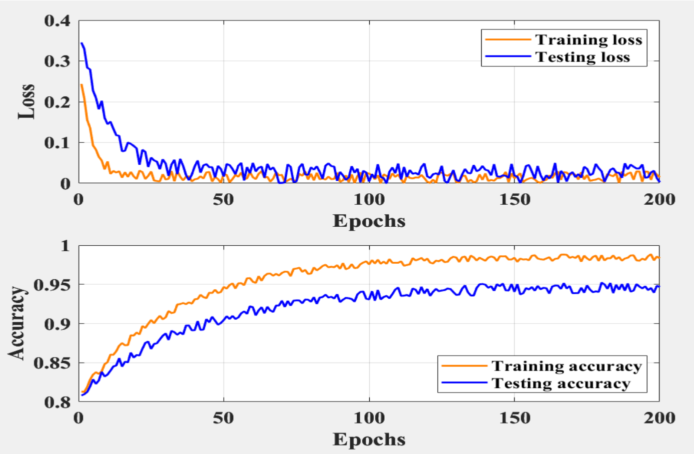

Figure 10: Training as well as testing performance

Figure 10 illustrates the training and testing performance of a model across 200 epochs. In the top plot, effective learning is indicated by the rapid drop in training and testing losses during the first epochs, followed by their stabilization near zero. In the bottom plot, the training and testing accuracies increase consistently with the number of epochs, demonstrating improved performance. The training accuracy reaches slightly higher values compared to testing accuracy, suggesting mild overfitting. Overall, the model achieves stable convergence with high accuracy and low loss, indicating strong generalization capability.

3.8.2. Performance analysis of the Warsaw Schizophrenia EEG dataset

The assessment results for the Warsaw Schizophrenia EEG dataset are presented below, with Table 4 comparing the proposed method's performance on this dataset.

Table. 5 Performance comparison of the suggested approach on the Warsaw Schizophrenia EEG dataset

Metrics / Methods	SzHNN [18]	SCAMBO-MVMKRVFLN [19]	VGG16-CNN [20]	MSST-Bi-CNN [21]	NHDETGCNets+QBANO (Proposed)
Accuracy (%)	95.2	96.1	93.2	92.8	**99.9**
Sensitivity (%)	93.9	90.5	89.4	91.5	**99.8**
Specificity (%)	91.5	92.8	90.3	88.9	**99.8**
Precision (%)	92.8	93.5	91.5	90.4	**99.8**
Recall (%)	90.6	88.7	91.7	93.8	**99.8**
F1- score (%)	89.8	91.5	90.7	92.8	**99.8**

Table 5 presents a performance comparison of various methods applied to the Warsaw Schizophrenia EEG dataset. The suggested NHDETGCNets+QBANO model performs better than current methods, attaining the best outcomes on every metric. In terms of accuracy, sensitivity, specificity, precision, recall, and F1-score, it records 99.9%, 99.8%, and 99.8%, respectively. Compared to prior models, such as SzHNN, SCAMBO-MVMKRVFLN, VGG16-CNN, and MSST-Bi-CNN, which achieved significantly lower performance, the proposed method demonstrates superior robustness, reliability, and efficiency. These results confirm the model's effectiveness in accurately predicting schizophrenia, minimising errors and surpassing earlier deep learning and hybrid approaches. Figure 11 shows the (a) Confusion matrix; (b) Correlation matrix.

The categorisation of healthy and paranoid schizophrenia participants is represented by a confusion matrix in Figure 11(a), where off-diagonal values denote incorrect classifications and diagonal values indicate accurate predictions. Specifically, 2 Healthy and 2 Paranoid Schizophrenia samples were correctly

ISSN: 2582 - 4201(Online) , http://www.ijrdes.com/ , IJRDES, Vol. 8, Issue 1, 2026 , https://doi.org/10.63328/IJRDES-V8RI1P3

identified, while 1 sample from each class was misclassified. Figure 11(b) depicts the correlation matrix between the classes, highlighting a positive correlation (1.00) along the diagonal and a negative correlation (-1.00) across different classes, signifying inverse relationships. Figure 12 shows the (a) Feature distribution and (b) class balance visualisation.

Figure 12 (a) illustrates the distribution of Feature1 values across healthy and paranoid schizophrenia groups, showing distinct segment allocations between the two classes. This highlights the variability of Feature1 and its contribution to separating the groups.

Figure 12(b) presents the class count distribution, demonstrating that both healthy and paranoid schizophrenia samples are well-balanced with equal representation. Such a balance ensures unbiased training and evaluation of classification models. Together, these plots emphasise the potential role of Feature1 in distinguishing between the two classes. Figure 13 shows the feature visualisation for the Healthy and Paranoid Schizophrenia groups.

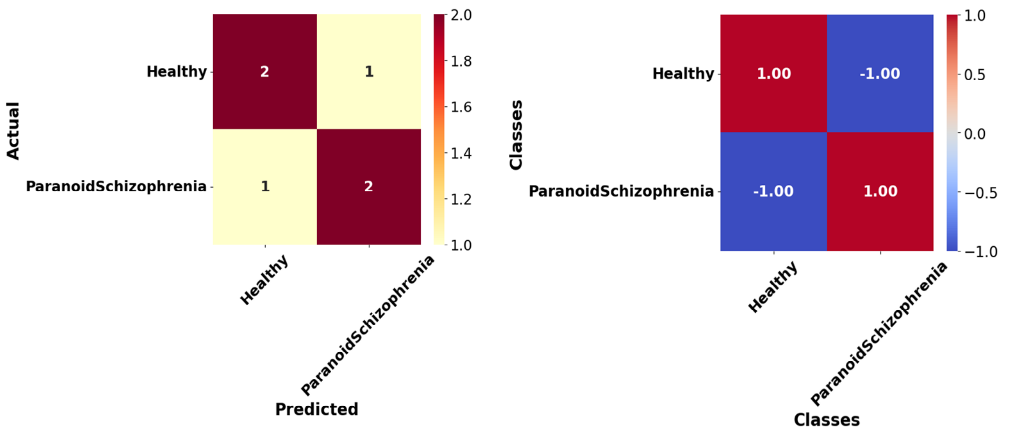

(a) (b)

Figure. 11 (a) Confusion matrix; (b) Correlation matrix

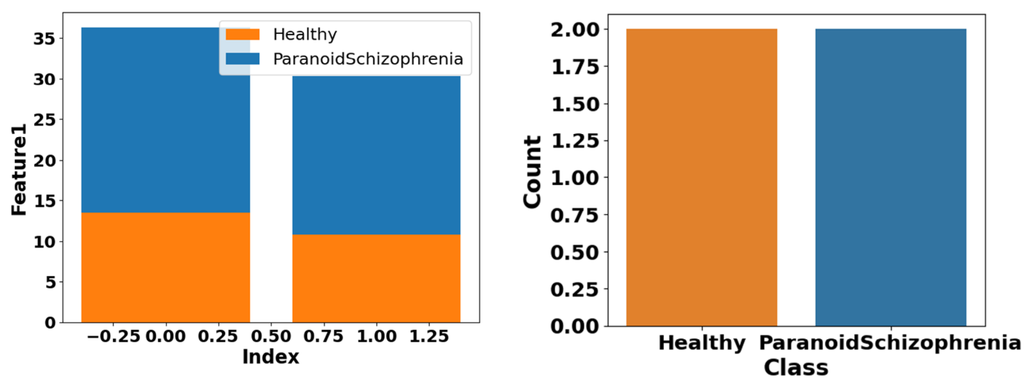

(a) (b)

Figure. 12 (a) Feature distribution and (b) class balance visualisation

Figure 13 demonstrates visual comparisons between the extracted features of Healthy and Paranoid Schizophrenia subjects. Subplot (a) shows the distribution of Feature1 across the two classes, indicating clear separation between Healthy (orange) and Paranoid Schizophrenia (blue). Subplot (b) highlights the relationship between Healthy Feature1 and Paranoid Schizophrenia Feature2, with a color intensity scale reflecting similarity values. Subplot (c) depicts the scatter plot of Feature1 versus Feature2, clearly distinguishing the two classes through clustering patterns. When taken as a whole, these visualisations highlight the ability of characteristics to discriminate, which helps with the precise categorization of individuals with schizophrenia in comparison to healthy controls. Figure 14 shows the feature 1 analysis for Healthy and Paranoid Schizophrenia subjects.

Figure 14 illustrates different analyses of Feature1 for Healthy and Paranoid Schizophrenia groups. Subplot (a) presents the trend of Feature1 values against the index, showing consistently higher values in the Paranoid Schizophrenia group compared to the Healthy group. Subplot (b) uses a violin plot to display the distribution and variability of Feature1 across the two classes, where

ISSN: 2582 - 4201(Online) , http://www.ijrdes.com/ , IJRDES, Vol. 8, Issue 1, 2026 , https://doi.org/10.63328/IJRDES-V8RI1P3

the Paranoid Schizophrenia group exhibits higher median values and a narrower spread than the Healthy group. Subplot (c) shows normalised frequency histograms of Feature1, highlighting a clear separation between the groups. Together, these plots confirm that Feature1 effectively differentiates Healthy individuals from schizophrenia patients. Figure 15 shows the (a) ROC curves, (b) Precision-Recall curves, (c) Error rate comparison,

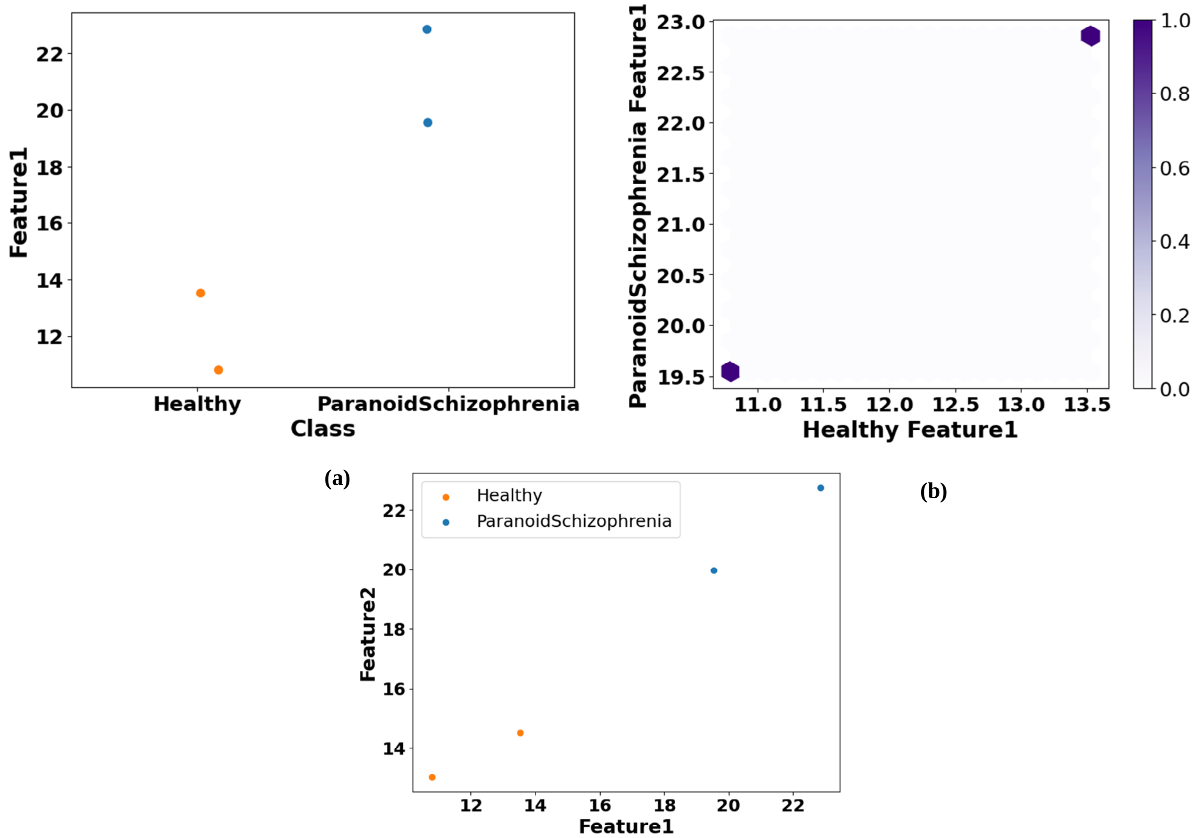

(a) (b) (c)

Figure. 13 Feature visualisation for Healthy and Paranoid Schizophrenia groups (a), (b), and (c)

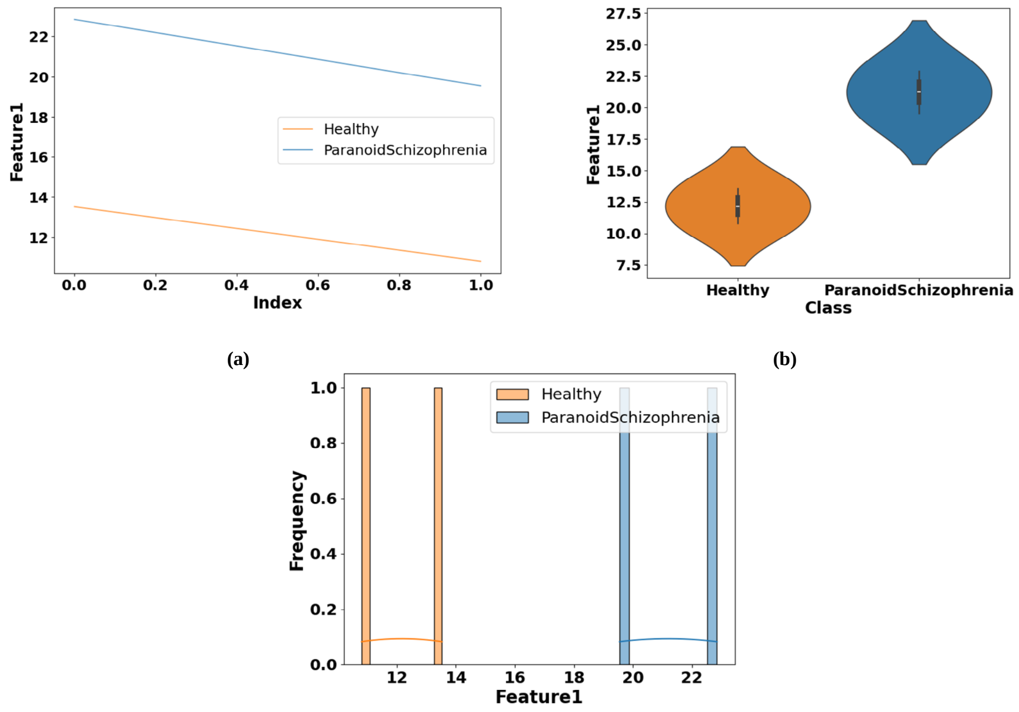

(a) (b) (c)

Figure. 14 Feature1 analysis for Healthy and Paranoid Schizophrenia subjects (a), (b), and (c)

ISSN: 2582 - 4201(Online) , http://www.ijrdes.com/ , IJRDES, Vol. 8, Issue 1, 2026 , https://doi.org/10.63328/IJRDES-V8RI1P3

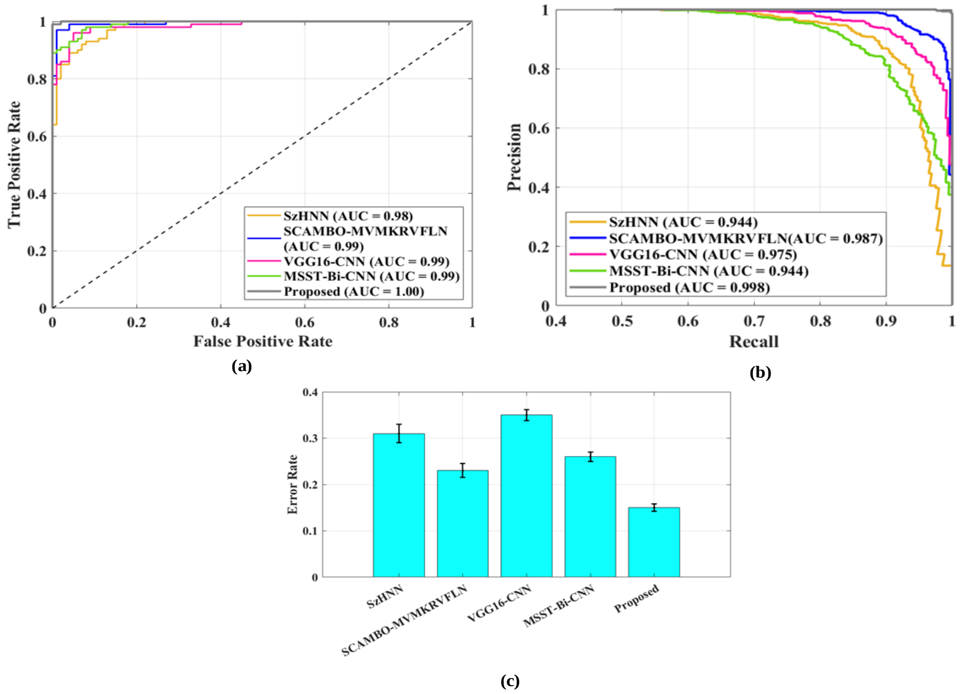

Figure. 15 (a) ROC curves, (b) Precision-Recall curves, (c) Error rate comparison

Figure 15 illustrates the performance evaluation of different models using ROC curves, Precision-Recall curves, and error rate comparison. The suggested model outperforms other models, such as SzHNN, SCAMBO-MVMKRVFLN, VGG16-CNN, and MSST-Bi-CNN in terms of classification accuracy, as evidenced by the ROC curve in subfigure (a), which displays the greatest AUC of 1.00. Subfigure (b) presents the Precision-Recall curve, where the proposed model outperforms others with the highest precision and recall values, indicating robust predictive capability. Subfigure (c) highlights the error rate comparison, where the proposed model achieves the lowest error rate, demonstrating its effectiveness and reliability for the given task. Figure 16 shows the training as well as the Testing Performance.

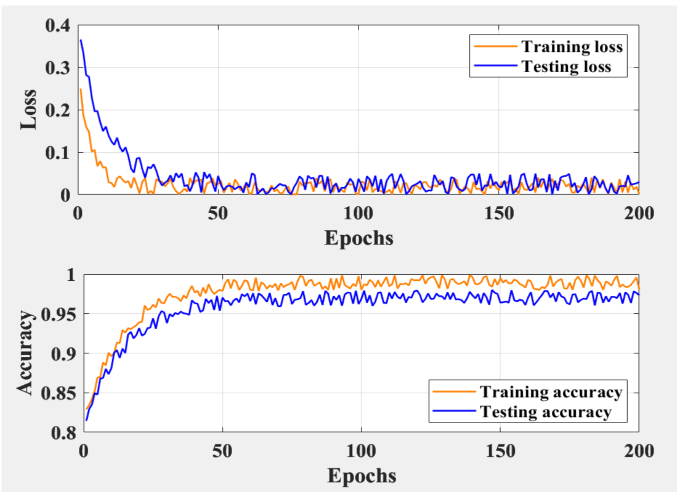

Figure. 16 Training as well as Testing Performance

Figure 16 illustrates the effectiveness of a deep learning model throughout 200 epochs of training and evaluation. The loss values are displayed in the top figure, where training and testing losses both drop very quickly in the early epochs before stabilising close to zero, signifying successful convergence. Accuracy is shown in the bottom plot; both training and testing accuracy increase gradually and surpass 97%, indicating a high capacity for generalisation. The training and testing curves' near alignment indicates that the model successfully prevents overfitting while retaining a high level of accuracy.

3.8.3. Performance comparison of the suggested method using both datasets

This section presents a comparison of the proposed methodology across the two datasets. Table 6 highlights the computation times and error rates achieved by various methods.

Table 6 compares different methods based on computational time and error rate. Traditional models, such as RNN-LSTM and CNN, along with their variants, exhibit computational times ranging from 0.70 to 0.88 seconds, with error rates varying from 6.4% to 8.8%. With the quickest calculation time of 0.20 seconds and the lowest error rate of 0.1%, the suggested NHDETGCNets+QBANO performs noticeably better than the others. This indicates that the proposed method is not only highly efficient but also more accurate, making it superior for tasks requiring both speed and precision in computation compared to conventional deep learning approaches.

ISSN: 2582 - 4201(Online) , http://www.ijrdes.com/ , IJRDES, Vol. 8, Issue 1, 2026 , https://doi.org/10.63328/IJRDES-V8RI1P3

Table. 6 Comparison of Methods Based on Computational Time as well as Error Rate

Method	Computational time (sec)	Error rate (%)
RNN-LSTM [16]	0.89	6.4
CNN [17]	0.70	7.6
SzHNN [18]	0.78	6.9
SCAMBO-MVMKRVFLN [19]	0.84	8.8
VGG16-CNN [20]	0.76	8.4
MSST-Bi-CNN [21]	0.85	8.7
Schizo-Net [22]	0.88	7.9
NHDETGCNets+QBANO (Proposed)	**0.20**	**0.1**

3.9. A Comparison of the Suggested Approach with Existing Techniques Statistically

Five statistical tests were employed to assess the effectiveness of the recommended strategy. Performance differences were evaluated using the Friedman test (FT), the Wilcoxon signed-rank test (WSR), and the Kruskal–Wallis H test. The data's normality was further evaluated using the Shapiro-Wilk (SW) and the Kolmogorov-Smirnov (KS) tests. Table 7 presents a comparative variance evaluation between the suggested technique and current approaches.

Table 7 compares the proposed NHDETGCNets+QBANO method with existing approaches (RNN-LSTM, CNN, SzHNN, SCAMBO-MVMKRVFLN, VGG16-CNN, MSST-Bi-CNN, Schizo-Net) across multiple statistical tests and performance metrics. Lower p-values in SW, WSR/U-test, H-test, KS test, and FT indicate NHDETGCNets+QBANO significantly outperforms others. It also demonstrates excellent accuracy and stability, achieving its smallest mean, standard deviation, and variance inflation factor. The suggested approach minimises error along with statistical uncertainty, while demonstrating improved dependability and decreased variability compared to previous models, indicating its efficacy for the intended application.

3.10. Ablation study of the suggested approach

An ablation study was conducted to evaluate the contribution of each component within the NHDETGCNets+QBANO framework. The results, presented in Table 8, highlight the overall effectiveness of the proposed approach and the performance improvements delivered by individual components.

Figure 8 illustrates the ablation study evaluating the impact of individual components AND-CTCN, HE-EGAN, and QBANO on model performance. The baseline model, without QBANO, achieves moderate results with an accuracy of 91.4%. When AND-CTCN or HE-EGAN are used independently, performance drops, highlighting their limited standalone effectiveness. Incorporating QBANO with either AND-CTCN or HE-EGAN significantly enhances F1-score, accuracy, recall, and precision. The full model, integrating all three components, achieves the highest performance with 99.9% across all metrics, demonstrating the complementary strengths and synergistic effect of the combined modules.

3.11. Discussion

The experimental findings and comparative evaluations clearly demonstrate the robustness and superiority of the proposed NHDETGCNets+QBANO framework for accurate SZ prediction using EEG data. By integrating advanced neural network design with optimised training via QBANO, the model achieved near-perfect classification performance across both the Moscow and Warsaw schizophrenia EEG datasets, significantly surpassing state-of-the-art approaches such as RNN-LSTM, CNN, SzHNN, SCAMBO-MVMKRVFLN, VGG16-CNN, and MSST-Bi-CNN. Notably, the proposed model consistently attained 99.9% accuracy, sensitivity, specificity, precision, recall, and F1-score, while simultaneously reducing computational time to 0.20 seconds and error rate to just 0.1%, establishing itself as both highly efficient and reliable. Visualisation analyses, including confusion matrices, correlation matrices, feature distributions, ROC and PR curves, and error rate comparisons, provided further evidence of its discriminative power and generalisation ability. The ROC and PR analyses, in particular, revealed AUC values of 1.00 and 0.997, respectively, confirming an exceptional classification capability with minimal false predictions. Statistical validation tests reinforced these findings, with significantly lower p-values indicating meaningful improvements over existing methods, while reduced variance inflation factors emphasized stability and reliability. Additionally, the ablation investigation emphasised the significance of every model element, showing that while AND-CTCN and HE-EGAN contributed positively, the synergy with QBANO was essential for achieving the observed superior results. Collectively, these outcomes emphasize the model's potential for practical applications in clinical neurodiagnostics, where both accuracy and computational efficiency are crucial for real-time decision support.

ISSN: 2582 - 4201(Online) , http://www.ijrdes.com/ , IJRDES, Vol. 8, Issue 1, 2026 , https://doi.org/10.63328/IJRDES-V8RI1P3

Table. 7 Statistical Comparison of the Suggested Approach with Existing Approaches

Methods	SW Test p-Value	WSR test / U-test p-Value	H-test p-Value	KS test p-value	FT p-Value	Mean	Standard Deviation	Variance Inflation Factor
RNN-LSTM [16]	0.427	0.364	0.86	0.087	0.088	278,730.79	3,330.20	1.79
CNN [17]	0.318	0.259	0.84	0.085	0.091	460,914.59	2,240.31	1.80
SzHNN [18]	0.349	0.168	0.94	0.083	0.084	81,807.39	3,185.45	1.83
SCAMBO-MVMKRVFLN [19]	0.450	0.249	0.86	0.089	0.077	384,923.85	2,370.52	1.94
VGG16-CNN [20]	0.387	0.375	0.90	0.078	0.075	282,458.57	1,163.40	1.84
MSST-Bi-CNN [21]	0.369	0.431	0.96	0.092	0.086	69,735.89	5,342.50	1.89
Schizo-Net [22]	0.296	0.312	0.93	0.081	0.087	66,813.39	1,322.13	1.75
NHDETGCNets +QBANO (Proposed)	<0.001	<0.001	<0.001	<0.001	<0.001	65,873.67	6,758.30	1.001

Table 8: Ablation study

Model Configuration	AND-CTCN	HE-EGAN	QBANO	Accuracy (%)	Precision (%)	Recall (%)	F1 Score (%)
Baseline (Without QBANO)	✓	✓	✗	91.4	90.2	92.6	90.4
AND-CTCN Only	✓	✗	✗	83.7	84.2	82.6	85.5
HE-EGAN Only	✗	✓	✗	85.7	86.8	80.3	86.8
AND-CTCN + QBANO	✓	✗	✓	92.5	91.7	90.4	90.9
HE-EGAN + QBANO	✗	✓	✓	91.8	88.5	87.6	89.4
Full Model NHDETGCNets+QBANO	✓	✓	✓	**99.9**	**99.8**	**99.8**	**99.8**

5. Conclusion

In this manuscript, the NHDETGCNets+QBANO framework is effectively implemented to achieve accurate prediction of schizophrenia. The input EEG signals from the Moscow and Warsaw schizophrenia datasets were first preprocessed using the AS-GLF technique, followed by feature extraction via the QQ-PFTD method. Prediction was then carried out using the NHDETGCNets model, which combines AND-CTCN with HE-EGAN. To enhance accuracy, reliability, and computational efficiency, the QBANO was employed for fine-tuning. The suggested model, fully implemented in Python, achieves outstanding predictive performance, delivering an impressive accuracy of 99.9% with a minimal error rate of only 0.1%. Future work could explore the incorporation of multimodal neuroimaging data, the development of real-time EEG-based detection of schizophrenia, the integration of explainable AI techniques, and the enhancement of model generalizability across diverse populations and clinical settings.

References

[1]. Bagherzadeh, Sara, Mohsen Sadat Shahabi, and Ahmad Shalbaf. "Detection of schizophrenia using hybrid of deep learning and brain effective connectivity image from electroencephalogram signal." *Computers in Biology and Medicine* 146 (2022): 105570.

ISSN: 2582 - 4201(Online) , http://www.ijrdes.com/ , IJRDES, Vol. 8, Issue 1, 2026 , https://doi.org/10.63328/IJRDES-V8RI1P3

[2]. Srinivasan, Sridevi, and Shiny Duela Johnson. "A novel approach to schizophrenia Detection: Optimized preprocessing and deep learning analysis of multichannel EEG data." *Expert Systems with Applications* 246 (2024): 122937.

[3]. Lamichhane, Bishal, Joanne Zhou, and Akane Sano. "Psychotic relapse prediction in schizophrenia patients using a personalized mobile sensing-based supervised deep learning model." *IEEE Journal of Biomedical and Health Informatics* 27.7 (2023): 3246-3257.

[4]. Luján, Miguel Ángel, et al. "Accurate neural network classification model for schizophrenia disease based on electroencephalogram data." *International Journal of Machine Learning and Cybernetics* 14.3 (2023): 861-872.

[5]. Ghanbari, Majed, Abdol Hamid Pilevar, and Narges Bathaeian. "Diagnosis of schizophrenia using brain resting-state fMRI with activity maps based on deep learning." *Signal, Image and Video Processing* 17.1 (2023): 267-275.

[6]. Yu, Tao, et al. "Prediction of violence in male schizophrenia using sMRI, based on machine learning algorithms." *Bmc Psychiatry* 22.1 (2022): 676.

[7]. Bretones, Carmen Soria, et al. "Automatic identification of schizophrenia employing EEG records analyzed with deep learning algorithms." *Schizophrenia Research* 261 (2023): 36-46.

[8]. Hassan, Fatima, Syed Fawad Hussain, and Saeed Mian Qaisar. "Fusion of multivariate EEG signals for schizophrenia detection using CNN and machine learning techniques." *Information Fusion* 92 (2023): 466-478.

[9]. Saadatinia, Mehrshad, and Armin Salimi-Badr. "An explainable deep learning-based method for schizophrenia diagnosis using generative data-augmentation." *IEEE Access* (2024).

[10]. Bracher-Smith, Matthew, et al. "Machine learning for prediction of schizophrenia using genetic and demographic factors in the UK biobank." *Schizophrenia research* 246 (2022): 156-164.

[11]. Barone, Annarita, et al. "Disorganization domain as a putative predictor of Treatment Resistant Schizophrenia (TRS) diagnosis: A machine learning approach." *Journal of Psychiatric Research* 155 (2022): 572-578.

[12]. Siuly, Siuly, et al. "SchizoGoogLeNet: The GoogLeNet-Based Deep Feature Extraction Design for Automatic Detection of Schizophrenia." *Computational Intelligence and Neuroscience* 2022.1 (2022): 1992596.

[13]. De Miras, J. Ruiz, et al. "Schizophrenia classification using machine learning on resting state EEG signal." *Biomedical Signal Processing and Control* 79 (2023): 104233.

[14]. Liu, Wenming, et al. "Graph-theory-based degree centrality combined with machine learning algorithms can predict response to treatment with antipsychotic medications in patients with first-episode schizophrenia." *Disease Markers* 2022.1 (2022): 1853002.

[15]. Gupta, Varun, et al. "An adaptive optimized schizophrenia electroencephalogram disease prediction framework." *Wireless Personal Communications* 130.2 (2023): 1191-1213.

[16]. Supakar, Rinku, Parthasarathi Satvaya, and Prasun Chakrabarti. "A deep learning based model using RNN-LSTM for the detection of schizophrenia from EEG data." *Computers in Biology and Medicine* 151 (2022): 106225.

[17]. Sobahi, Nebras, et al. "A new signal to image mapping procedure and convolutional neural networks for efficient schizophrenia detection in EEG recordings." *IEEE Sensors Journal* 22.8 (2022): 7913-7919.

[18]. Sharma, Geetanjali, and Amit M. Joshi. "SzHNN: A novel and scalable deep convolution hybrid neural network framework for schizophrenia detection using multichannel EEG." *IEEE Transactions on Instrumentation and Measurement* 71 (2022): 1-9.

[19]. Parija, Sebamai, et al. "Autoencoder-based improved deep learning approach for schizophrenic EEG signal classification." *Pattern Analysis and Applications* 26.2 (2023): 403-435.

[20]. Aslan, Zülfikar, and Mehmet Akin. "A deep learning approach in automated detection of schizophrenia using scalogram images of EEG signals." *Physical and Engineering Sciences in Medicine* 45.1 (2022): 83-96.

[21]. Jindal, Komal, et al. "Bi-LSTM-deep CNN for schizophrenia detection using MSST-spectral images of EEG signals." *Artificial Intelligence-Based Brain-Computer Interface*. Academic Press, 2022. 145-162.

[22]. Grover, Nitin, et al. "Schizo-Net: A novel Schizophrenia Diagnosis framework using late fusion multimodal deep learning on Electroencephalogram-based Brain connectivity indices." *IEEE Transactions on Neural Systems and Rehabilitation Engineering* 31 (2023): 464-473.

[23]. Ajmeera, Narahari, and P. Kamakshi. "Hamiltonian deep neural network fostered sentiment analysis approach on product reviews." *Signal, Image and Video Processing* 18.4 (2024): 3483-3494.

[24]. Hitzer, Eckhard. "Quadratic Phase Quaternion Domain Fourier Transform." *Computer Graphics International Conference*. Cham: Springer Nature Switzerland, 2023.

[25]. Ren, Xiaoying, et al. "A novel dual-channel temporal convolutional network for photovoltaic power forecasting." *Energies* 17.3 (2024): 698.

[26]. Mo, Xiaoyu, et al. "Multi-agent trajectory prediction with heterogeneous edge-enhanced graph attention network." *IEEE Transactions on Intelligent Transportation Systems* 23.7 (2022): 9554-9567.

[27]. Fatahi, Ali, Mohammad H. Nadimi-Shahraki, and Hoda Zamani. "An improved

ISSN: 2582 - 4201(Online) , http://www.ijrdes.com/ , IJRDES, Vol. 8, Issue 1, 2026 , https://doi.org/10.63328/IJRDES-V8RI1P3

binary quantum-based avian navigation optimizer algorithm to select effective feature subset from medical data: a COVID-19 case study." *Journal of Bionic Engineering* 21.1 (2024): 426-446.

Declaration

Conflicts of Interest: The authors declare no conflict of interest.

Author Contribution: All authors wrote the main manuscript text and also consent to the submission.

Ethical approval: Not applicable.

Consent to Participate: All authors consent to participate.

Funding: Not applicable, and No funding was received

Institutional Review Board Statement: Not applicable.

Informed Consent Statement: Not applicable.

Personal Statement: We declare with our best of knowledge that this research work is purely Original Work and No third party material used in this article drafting. If any such kind material found in further online publication, we are responsible only for any judicial and copyright issues.

Acknowledgements

We thank everyone who inspired our work.